THERMOELECTRIC BASED TEMPERATURE CONTROL BOX FOR QCM SENSOR MEASUREMENT CELL

Setyawan Purnomo Sakti*, Putri Surya Arinda, and Ridha Novani Ikhsani

Received: December 14, 2018; Revised: February 19, 2019; Accepted: February 28, 2019

Abstract

The QCM sensor has a sensitivity to the viscosity and density change of the liquid in contact with the sensor. As the viscosity and density of a liquid are usually temperature dependent, temperature stability of the liquid is an important point in the QCM measurement related to the liquid viscosity and density. In an application, the temperature needs to be maintained constant along with the measurement process. In the impedance-based measurement of the QCM sensor in contact with liquid, the temperature needs to be maintained in its constant value during the measurement process. A circulating water bath was commonly used. The disadvantages of the system were high energy consumption and slow response. In this work, the thermoelectric element was used to maintain the temperature of the sensor and the liquid being measured. Three thermoelectric modules were used and independently controlled to provide a temperature profile to the QCM sensor module. The chamber temperature was measured using a thermistor to be used as a feedback signal to control the thermoelectric current. The measurement showed that the temperature of the thermoelectric surface was inhomogeneous. Small temperature variation on the surface was observed. However, the results showed that the temperature stability of the QCM sensor chamber and liquid could be maintained with 0.2ºC stability. Temperature control was done by controlling the pulsed DC current to the thermoelectric. This method allows the temperature change of the liquid sample on top of the QCM sensor by 5ºC/min at still air.

Keywords: Thermoelectric; temperature control; temperature distribution; QCM measurement

---

Department of Physics, Faculty of Mathematics and Natural Science, Brawijaya University, Jl Veteran, Malang 65145, Indonesia. E-mail: sakti@ub.ac.id

* *Corresponding author*

Introduction

Quartz Crystal Microbalance is one from many sensors which sensitively respond to the viscosity and density of the liquid in contact with the sensor. The respond of the sensor to the viscosity and density of the contacting medium was described by Kanazawa and Gordon (Keiji Kanazawa and Gordon, 1985). This understanding was not only used as a basis for the QCM application for measuring in liquid viscosity but also became a valuable knowledge for the QCM measurement for many application (Saluja and Kalonia, 2004; Wang *et al*., 2005; Luo *et al*., 2006; Tan and Huang, 2013; Choi *et al*., 2014; Salama *et al*., 2014).

QCM sensor measurement can be done using an oscillator, impedance, and decay based measurement (Alassi *et al*., 2017). Every measurement method has its advantages and disadvantages related to the measurement complexity and collected data to be processed. Oscillator and decay based measurement provide a rapid measurement for a given time and are usually used to measure a reaction process which requires a long time acquisition to follow the process. The impedance measurement provides the best method to give a set of data for a complex measurement where comprehensive data is taken at a given condition by an assumption that the condition remains during the measurement process. However, to get an accurate measurement, the acquisition process usually takes several min long. Typical impedance measurement speed is 10 ms to 1s per point. Higher measurement accuracy required longer measurement time. Using Bode 100 Impedance Analyser, we required an acquisition time of 10 min for accurate measurement of 4,096 points. This leads to a condition where the assumption of a constant condition of the measurement was not easily achieved.

For the liquid measurement, all the measurement methods need a constant temperature condition of the sensor and liquid sample. In other experiments, the temperature of the liquid and sensor was set at a given temperature by intention for the study (Martin *et al*., 1997; Cao-Paz *et al*., 2012). Therefore temperature control for the chamber reaction was needed. A typical method used a circulating water bath, resistive element heating, and thermoelectric with heat capacitive block.

Quartz crystal microbalance sensor has a small physical dimension. The quartz size has a diameter of 8.7 mm to 25 mm. The reaction chamber usually ranges from several centimeters in width, length, and height. For a small reaction chamber, the use of thermoelectric to control the temperature has many advantages such as low energy consumption, less noise, less mechanical vibration, fast response time, simple control system (Riffat and Ma, 2003; Mannella *et al*., 2014) and easy placement with orientation freedom. The power consumption can be less than 15 watts for a small chamber, comparing to a water heater/cooler which consumes hundred to thousand watts. The noise from the thermoelectric heater/cooler was only from the used fan which can be less than 15 dBA. The response time of the thermoelectric element can be less than 5 sec (Semeniouk and Pilipenko, 1996) comparing to a circulating water bath which requires more than 10 min (Verma *et al*., 2012).

The thermoelectric as cooler and heater can be controlled using a simple classical method to intelligent control (Thakor *et al*., 2015; Peronio *et al*., 2017; Cai *et al*., 2019; He *et al*., 2019). Among many different control methods, an on-off control and pulse width modulation to deliver a current to the thermoelectric module as a cooler and heater is one of the simplest methods. The current pulse is known as an effective method to control a thermoelectric module for cooling (Nagy and Roman, 1999; Snyder *et al*., 2002; Ma *et al*., 2015; Cai *et al*., 2016). The current pulse was also easy to be implemented using electronic devices. This work aims to develop a simple thermoelectric based temperature control box to be used to maintain constant room temperature for a small QCM sensor. The temperature profile of the thermoelectric module was observed during the cooling

process. The temperature measurement used a small thermistor sensor. The measurement process and control action was done using an 8-bit microcontroller. The surface temperature distribution of the thermoelectric module was measured using a thermal camera.

Materials and Methods

Thermoelectric Module

The thermoelectric module is TEC1-12706 which was made of Bismuth Telluride (Bi_2Te_3) semiconductor. The module was placed between alumina (Al_2O_3) substrate with a dimension of 40×40 mm. The modules have a maximum temperature difference of 70ºC. The resistivity of the module is 1.98º to 2.3º. The thermoelectric can be driven with a maximum current of 6A and a maximum voltage of 16.4Volt.

QCM Sensor and the Sensor Cell

The QCM sensor was an AT-Cut crystal resonator with the HC-49/U form factor. The crystal resonator has a diameter of 8.7 mm and 5 mm silver electrode. It was purchased from PT Great Microtama, Surabaya, Indonesia. The sensor had a series resonance frequency of 10MHz. The cell reaction of the sensor was made using the 3D printer with ABS plastic mold material. When the sensor was installed in the reaction cell, there was a cylindrical chamber with a diameter of 6mm on top of the QCM sensor. It allowed an amount of liquid sample up to 50µL. The sensor cell outer dimension was 35×35×10 mm. Figure 1 shows the picture of the QCM sensor cell and the sensor inside the cell.

Thermistor for Temperature Measurement

The electronic devices for measuring the temperature of the reaction cell and thermoelectric was a thermistor NTC B3950 with a resistance of 10KΩ and tolerance of 1%. The thermistor head was made of a small size glass bead with a diameter of 1.25 mm and length of 2.0 mm. The thermistor power dissipation coefficient at still air was higher 5 mW/°C with a maximum power of 45 mW. Thermal time coefficient was less than 7 s in still air. The heat capacity of the thermistor head was less than 7 mW/K. The resistance of the thermistor was measured based on a voltage divider circuit of the thermistor and 10KΩ resistance. The temperature was calculated using the Steinhart-Hart Equation:

$$T = \left(\frac{1}{A+B\ln R+C(\ln R)^3} - 273.15\right)^o C \qquad (1)$$

where
$A = 1.009249522\times10^{-3}$,
$B = 2.378405444\times10^{-4}$ and
$C = 2.019202697\times10^{-7}$.

The Current Driver for the Thermoelectric

The thermoelectric current was driven by using L2984N H-Bridge. In this work, the current to the thermoelectric through the driver was in the form of pulse width modulated current with a frequency of 31.25 kHz. The source of the DC current was a DC power supply with an output rate of 5VDC and 5 A. Based on the thermoelectric module specification, at 5VDC the current flow in the module was 2.5 A or less. With the pulse DC current, the effective current to the thermoelectric was less than 2 A.

The Thermoelectric Temperature Control Box

The thermoelectric temperature control box was a cubical box with the wall dimension of 40 mm length and 40 mm width. The wall made of the thermoelectric module and acrylic

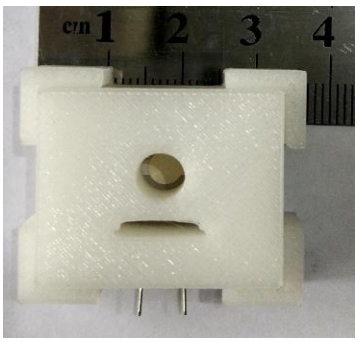

Figure 1. QCM sensor cell

sheet with a thickness of 5 mm. Figure 2 shows the thermoelectric temperature control box. The thermistor head was placed on each of the thermoelectric. One thermistor head (in the middle) was placed in the QCM cell.

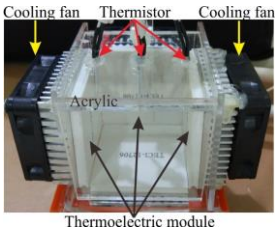

(a)

(b)

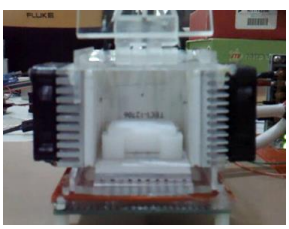

Figure 2. Thermoelectric temperature control box with a cooling fan on each active thermoelectric module. (a) front view, (b) top view, (c) front view with QCM cell inside

System Block Diagram

The overall system block diagram can be seen in Figure 3. The core of the control system was an ATMega328 microcontroller. The voltage of the thermistor sensor circuit was connected into the 10 bit analog to digital converter (ADC) of the microcontroller. The sensors measured the temperature close to the thermoelectric module surface, the temperature in the QCM cell, and the temperature outside of the box.

Based on the temperature of the QCM cell and the targeted temperature, the microcontroller activated the PWM control to the current driver (L298N). The duty cycle of the PWM working at 31.25KHz was set in the microcontroller code. The simple on-off control was used to maintain the QCM cell temperature at a constant temperature. If the temperature of the QCM cell was higher than the targeted temperature, the PWM was activated until the temperature was less than the targeted temperature.

Surface Temperature Measurement

Surface temperature measurement of the thermoelectric module was carried out using IR camera Fluke TIS20. The temperature measurement resolution was 0.1ºC. The surface temperature measurement of the thermoelectric module was taken from a distance of 30 cm. Thermal image post-processing and thermal data extraction were done using Fluke Thermal Image Editor software.

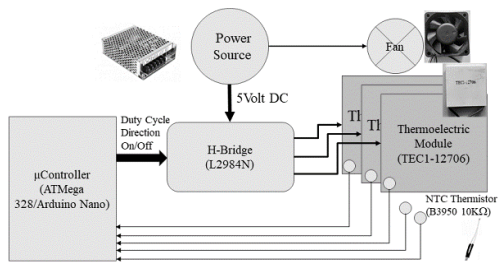

Figure 3. Overall electronic system circuit for the thermoelectric temperature control box

Results and Discussion

Surface Temperature of the Thermoelectric Module

The measured temperature surface of the thermoelectric during a heating state and cooling state can be seen in Figure 4. The temperature is presented in an RGB color from red indicating high temperature to blue indicating cool temperature. The color scale bar was set from 20ºC to 50ºC.

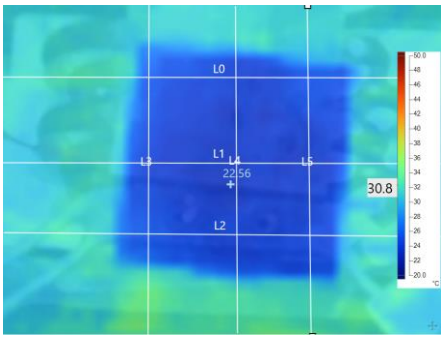

(a)

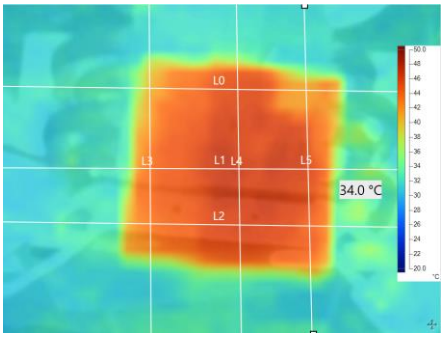

(b)

Figure 4. A surface temperature of the thermoelectric module at cooling (a) and heating (b) stage

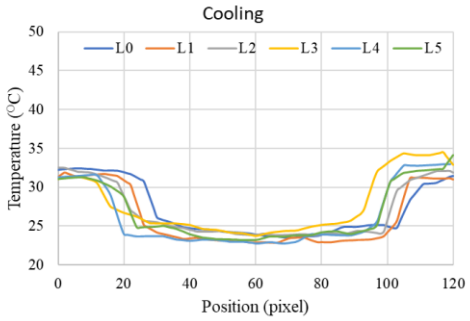

(a)

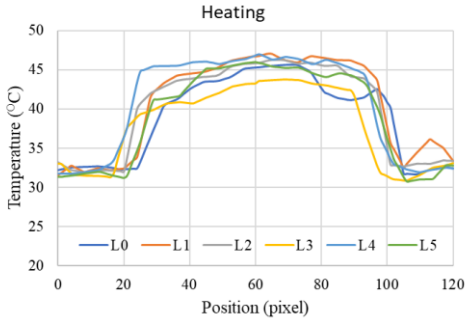

(b)

Figure 5. The temperature profile of the thermoelectric module at cooling (a) and heating (b) stage

It can be seen that the surface temperature of the module was varied. In the cooling stage, the color of the thermoelectric module was blue. The temperature was lower than the ambient temperature around the thermoelectric module. The surface temperature at the edge was brighter than in the middle, indicating that the edge temperature was higher than the temperature in the middle. However, the surface temperature color was not perfectly blue. It indicated that there was also a temperature variation on the module surface, even in the middle of the module. In the heating stage, the temperature was higher than the surrounding temperature indicated by a color close to red. Similar to the condition at the cooling stage, the temperature of the surface was inhomogeneous. At the edge of the module, the temperature was lower.

Figure 5 shows the temperature profile of the thermoelectric module taken at the given line indicated by L0, L1, L2, L3, L4, and L5. The profile shows a dramatic change in the temperature between the thermoelectric module, and it's surrounding around image pixel number 20 and 100. Based on thermoelectric dimension, the pixel size of the temperature image is equivalent to around 0.5 mm. Figure 6 focuses on the area of the thermoelectric module. It can be seen that the temperature variation around the thermoelectric surface center was about 1°C. This temperature variation affects heat radiation the thermoelectric module to its surrounding area. Therefore it is also possible that the surrounding area temperature is also varied. The variation of the surface temperature of the module was attributed to the location distribution of the semiconductor cell (Mannella *et al*., 2014). It was known that the semiconductor of the thermoelectric cell was placed with a spacing.

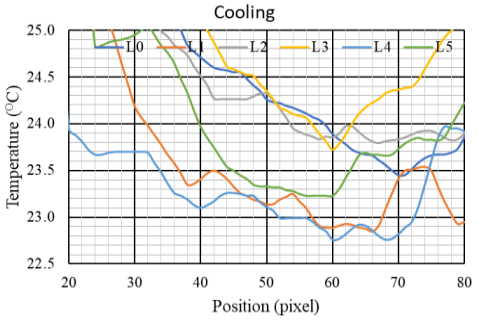

(a)

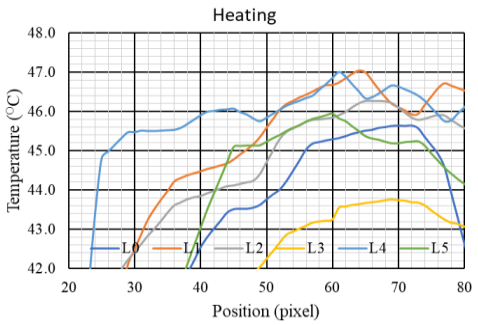

(b)

Figure 6. The temperature profile of the thermoelectric module in the middle during cooling (a) and heating (b) stage

PWM Effect to the Cooling and Thermoelectric Surface Temperature

The thermoelectric as a cooling or heating device could be controlled by delivering a constant DC current or DC pulse current. The direction of the current flow set the cool and hot side of the thermoelectric. For a cooler box, the hot side was placed outside of the box. The performance of the thermoelectric as a cooler was supported by placing a heat pipe or fan on the hot side. In this design, we used a pulsed DC current controlled by a PWM system with different duty cycle. For the cooling, a 40 mm fan was placed at the hot side of the thermoelectric as depicted in Figure 2.

Pulse DC current was selected as it was known to be the best method to drive the thermoelectric as a cooler. Although with the constant current, the surface temperature of the thermoelectric module as the cooler also varied with time because of the heat transfer between the cold side and hot side, and Peltier cooling process (Ma *et al*., 2015). As the effective current related to the power, it was expected that a high duty cycle would result in faster cooling speed.

Figure 7 shows the temperature inside of the thermoelectric temperature control box and outside temperature as well as the working state of the thermoelectric. At the on state, the thermoelectric was working as a cooler, while at off state, the thermoelectric was at idle state. At on state, the pulse DC current was flowing to the thermoelectric modules. At idle state, no current flowed to the modules. The duty cycle of the PWM has been set from 7.8% to 39.2%.

It can be seen that the temperature close to the thermoelectric module surface is lower than the temperature at the QCM cell. It is related to the fact that the thermoelectric worked as a cooling part. As there was no air flow, and the thermal conductivity of air at room temperature was very low (0.0262 W/mK), the heat conduction and convection were negligible. The heat transfer from the QCM sensor cell to the thermoelectric surface was mainly caused by the radiation (Luo *et al*., 2016). The temperature change in the thermolectric surface was immediately followed by the temperature change in the thermistor at the QCM cell. The temperature difference between the thermoelectric surface and the QCM cell was also significant as the air itself behaves as a thermal insulator. In addition, it can be seen that the thermoelectric surface temperature differed one to others. This shows radiation and heat absorption that is not evenly distributed between thermoelectric cells.

At low duty cycle, which means a lower effective current, the thermoelectric temperature cannot go too low. The absorbed heat from the QCM cell and heat radiated from the outside temperature through the acrylic window could not be handled by the thermoelectric. The temperature of the QCM cell reached its target temperature setting from 23°C to 25°C (below outside temperature) when the PWM duty cycle higher or equals to 31.4%. At higher duty

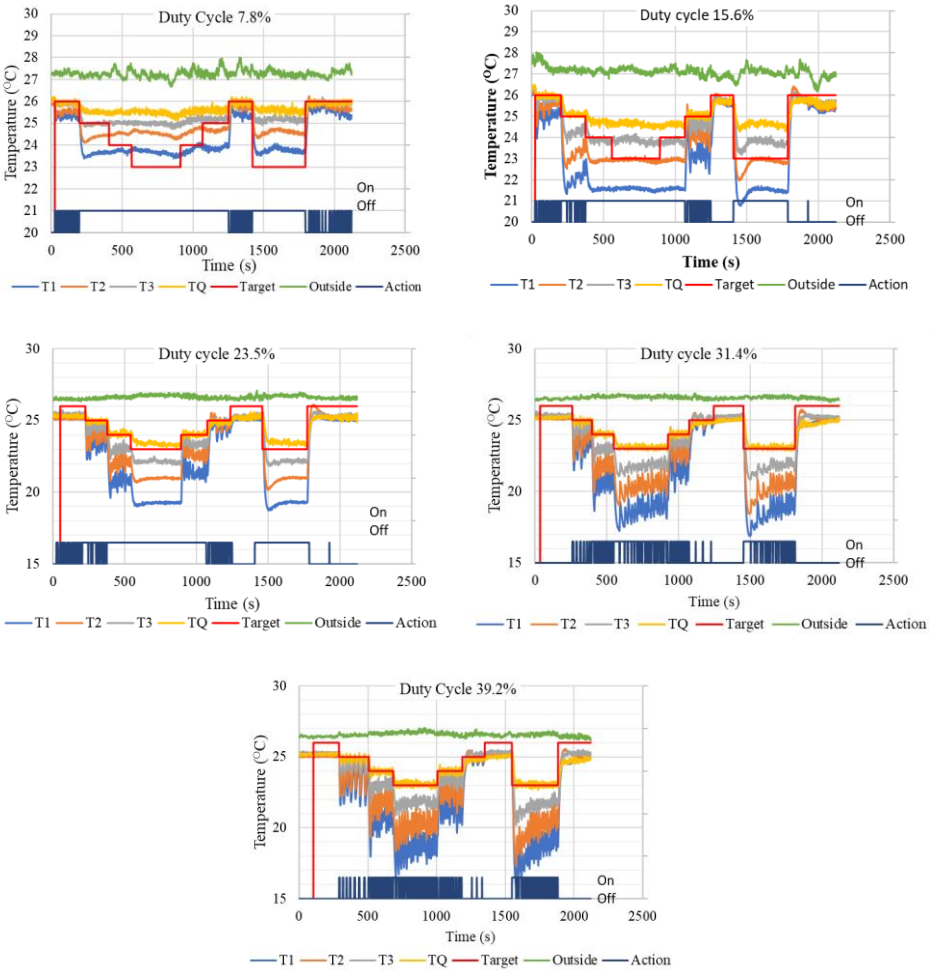

Figure 7. The temperature at the thermoelectric surface (T1, T2, T3), QCM cell (TQ), and outside temperature (outside), and a target temperature of the QCM cell. The dark blue line is indicating the on-off control state of the thermoelectric

cycle, the temperature of the thermoelectric can go lower enough to absorb heat from the QCM cell and heat radiated from outside the chamber through the acrylic wall. The temperature profile of the thermoelectric surface and the QCM cell was similar at duty cycle 31.4% and 39.2%.

Temperature Response and Stability of The QCM Cell

The response time of the thermoelectric temperature control box can be seen in Figure 8. The temperature changed from 25°C to 24°C and 24°C to 23°C according to the target temperature within 11 to 16 sec. The temperature change was equal to 5°C/min.

As the thermoelectric in the cooling stage, the temperature of the thermoelectric went down followed by the QCM cell temperature. The delay time in the temperature between the thermoelectric module surface and the QCM cell was around 2-3 sec. Considering that the distance of the thermoelectric surface and the center of the

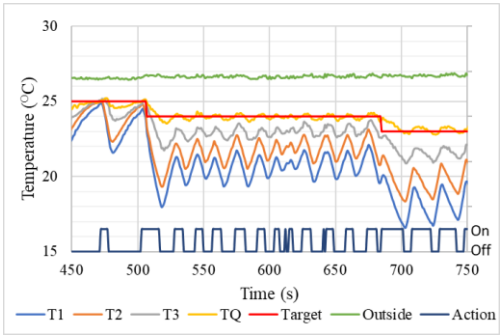

Figure 8. Response time and temperature variation of the thermoelectric module

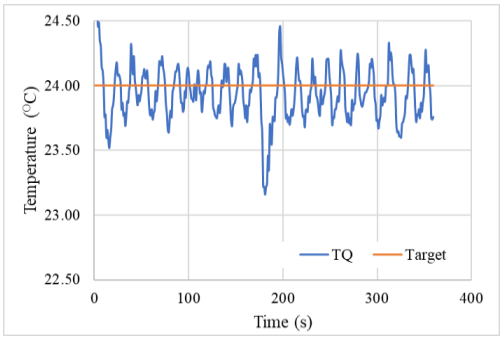

Figure 9. Temperature stability at QCM cell

QCM cell was 20 mm, it indicated that the heat transfer through the radiation played a more important role than the conduction through the still air.

The temperature variation of the thermoelectric temperature which followed the on-off control action can be attributed to the heat transfer from the hot side to the cold side of the thermoelectric. When there was no electric current into the thermoelectric, the heat was transfer through conduction from the hot side to cold side. It was indicated by increasing the temperature of the thermoelectric surface inside the box (as the cold side). When the current was flowing, the temperature was decreased. This behavior showed that the radiative cooling using the thermoelectric module was varied by time dynamically (Luo *et al*., 2016).

The temperature gradient of the thermoelectric surface during the on state and off state was from 1°C to 3°C at constant targeted temperature. The temperature gradient resulted in a high-temperature variation at the QCM cell as seen in Figure 9. The temperature of the QCM cell fluctuated following the temperature change of the thermoelectric. At a targeted temperature of 24°C, the QCM cell temperature was 24.0°C±0.2.

Conclusions

Thermoelectric temperature control box for the QCM sensor cell reaction has been successfully developed using three thermoelectric modules. The temperature distribution of the thermoelectric surface was varied at around 1°C in the middle of the module. Significant temperature gradient occurred at the edge of the thermoelectric module. Using a pulsed DC current, on-off control and PWM modulation the thermoelectric module able to control the temperature inside the box when the PWM duty cycle was higher or equal to 31.4%. The thermoelectric surface temperature rapidly changed between the active and idle state caused by the heat transfer from the hot side to the cold side. The variation of thermoelectric temperature was quickly followed by the temperature variation of the QCM cell. Using the on-off control and PWM with a duty cycle of 39.2%, the temperature variation of the QCM cell was 0.2°C.

Acknowledgment

This work was part of a research project funded by the Ministry of Research, Technology and Higher Education of the Republic of Indonesia research grant scheme.

References

Alassi, A., Benammar, M., and Brett, D. (2017). Quartz crystal microbalance electronic interfacing systems: A review. Sensors, 17(12):1-41.

Cai, Y., Liu, D., Zhao, F.Y., and Tang, J.F. (2016). Performance analysis and assessment of

thermoelectric micro cooler for electronic devices. Energy Convers. Manag., 124:203–211.

Cai, Y., Wang, Y., Liu, D., and Zhao, F.Y. (2019). Thermoelectric cooling technology applied in the field of electronic devices: Updated review on the parametric investigations and model developments. Appl. Therm. Eng., 148:238-255.

Cao-Paz, A.M., Rodríguez-Pardo, L., Fariña, J., and Marcos-Acevedo, J. (2012). Resolution in QCM sensors for the viscosity and density of liquids: Application to lead-acid batteries. Sensors, 12(8):10,604-10,620.

Choi, J., Kanazawa, K.K., and Cho, N. (2014). Effect of a Non-Newtonian Load on Signature S2 for Quartz Crystal Microbalance Measurements. J. Sensors, 2014:1–8.

He, H., Liu, W., Wu, Y., Rong, M., Zhao, P., and Tang, X. (2019). An approximate and efficient characterization method for temperature-dependent parameters of thermoelectric modules. Energy Convers. Manag., 180:584-597.

Keiji Kanazawa, K. and Gordon, J.G. (1985). The oscillation frequency of a quartz resonator in contact with liquid. Anal. Chim. Acta., 175:99-105.

Luo, Y., Chen, M., Wen, Q., Zhao, M., Zhang, B., Li, X., Wang, F., Huang, Q., Yao, C., Jiang, T., Cai, G., and Fu, W. (2006). Rapid and Simultaneous Quantification of 4 Urinary Proteins by Piezoelectric Quartz Crystal Microbalance Immunosensor Array. Clin. Chem., 52(12):2,273-2,280.

Luo, Y., Zhang, L., Liu, Z., Wang, Y., Meng, F., and Xie, L. (2016). Modeling of the surface temperature field of a thermoelectric radiant ceiling panel system. Appl. Energy, 162:675-686.

Ma, M., Yu, J., and Chen, J. (2015). An investigation on thermoelectric coolers operated with continuous current pulses. Energy Convers. Manag., 98:275-281.

Mannella, G.A., La Carrubba, V., and Brucato, V. (2014). Peltier cells as temperature control elements: Experimental characterization and modeling. Appl. Therm. Eng., 63(1):234-245.

Martin, S.J., Spates, J.J., Wessendorf, K.O., Schneider, T.W., and Huber, R.J. (1997). Resonator/Oscillator Response to Liquid Loading. Anal. Chem., 69(11):2,050-2,054.

Nagy, M.J. and Roman, S.J. (1999). The effect of pulse width modulation (PWM) frequency on the reliability of thermoelectric modules. In Eighteenth International Conference on Thermoelectrics. Proceedings, ICT'99 (Cat. No.99TH8407), IEEE., p. 123-125.

Peronio, P., Labanca, I., Ghioni, M., and Rech, I. (2017). Note: Wide-operating-range control for thermoelectric coolers. Rev. Sci. Instrum., 88(11):116102.

Riffat, S.B. and Ma, X. (2003). Thermoelectrics: A review of present and potential applications. Appl. Therm. Eng., 23(8):913-935.

Salama, I.E., Binks, B.P., Fletcher, P.D.I., and Horsup, D.I. (2014). Adsorption of benzyldimethyldodecyl-ammonium chloride onto stainless steel using the quartz crystal microbalance and the depletion methods: An optimization study. Colloids Surfaces A Physicochem. Eng. Asp., 447:155-165.

Saluja, A., and Kalonia, D. S. (2004). Measurement of fluid viscosity at microliter volumes using quartz impedance analysis. AAPS Pharm. Sci. Tech., 5(3):68-81.

Semeniouk, V.A. and Pilipenko, T.V. (1996). Thermoelectric coolers with small response time. In Fifteenth International Conference on Thermoelectrics. Proceedings ICT '96, IEEE., p. 301-306.

Snyder, G.J., Fleurial, J.P., Caillat, T., Yang, R., and Chen, G. (2002). Supercooling of Peltier cooler using a current pulse. J. Appl. Phys., 92(3):1,564-1,569.

Tan, F. and Huang, X.H. (2013). Relations between mass change and frequency shift of a QCM sensor in contact with viscoelastic medium. Chinese Phys. Lett., 30(5).

Thakor, M.D., Hadia, S.K., and Kumar, A. (2015). Precise temperature control through Thermoelectric Cooler with PID controller. 2015 Int. Conf. Commun. Signal Process. ICCSP 2015, p. 1,118-1,122.

Verma, O.P., Singla, R., and Kumar, R. (2012). Intelligent Temperature Controller for Water Bath System. World Acad. Sci. Eng. Technol. Int. J. Comput. Information, Syst. Control Eng., 6(9):1,232-1,238.

Wang, D., Mousavi, P., Hauser, P.J., Oxenham, W., and Grant, C.S. (2005). Quartz crystal microbalance in elevated temperature viscous liquids: Temperature effect compensation and lubricant degradation monitoring. Colloids Surfaces A Physicochem. Eng. Asp., 268(1-3):30-39.